Discovery of Evidence for Correlated X-ray/GeV Variability in the Feb 2010 Flare of Mrk 421

G. Madejski[1], J. Chiang[1], S. Fegan[2], B. Giebels[2] & D.Horan[2]
on behalf of the *Fermi*-LAT collaboration

[1] KIPAC, SLAC National Accelerator Laboratory, Menlo Park, CA, USA
[2] Laboratoire Leprince Ringuet / Ecole Polytechnique, Palaiseau, France

2012 AAS, 08-12 January 2012, Austin, Texas

Abstract: The high-synchrotron-peaked BL Lac (HBL) Markarian 421 was observed during a bright X-ray flaring period in February 2010, in the GeV band by the *Fermi* Large Area Telescope, and in X-rays by the RXTE, *Swift*, and MAXI observatories. For the first time in a HBL, we find evidence for correlated variability between the X-ray and GeV emission. Including data from the UVOT instrument aboard *Swift*, we model the spectral energy distribution of the source in the pre-flare, flare and post-flare time periods using a standard synchrotron self-Compton (SSC) model. In the context of these models, the GeV and X-ray emission arise from electrons with significantly different energies in the particle distributions that are inferred from the models.

1. Analysis of the multi-wavelength data:

This study focusses on a well-defined X-ray flare from Mrk 421, which peaked on MJD 55243 (2010 Feb 16). The HE gamma-ray flux measured with the *Fermi*-LAT was sufficiently high that a daily-binned light curve could be derived. In X-rays, the MAXI data provide the best temporal sampling, while the X-ray spectrum was derived from the public *Swift*-XRT data.

The *Fermi*-LAT data were analyzed using a binned maximum-likelihood method as implemented in the *ScienceTools* package, using the P7SOURCE_V6 event selection and instrument response functions. We analyzed events with energies between 100 MeV and 100 GeV from a 10° region of interest (ROI) around Mrk 421. To reduce contamination from atmospheric gamma rays only events with a reconstructed zenith angle of less than 100° were considered. A model for the emission in the ROI was constructed, including all 2FGL point sources in the ROI [1], from which the parameters of a power-law (PL) fit to the spectrum of Mrk 421 were extracted. A light curve was produced by binning the data during the 24-day period surrounding the flare into 1-day time periods. The spectral evolution of the source during the flare was evaluated by dividing the data into three 4-day time periods, as discussed in Section 2, and calculating the parameters of the best-fit PL spectrum in each period.

Given the high X-ray flux, the XRT observations were made in windowed observation mode to avoid pileup effects. The data were reduced with the HEASOFT 6.11 package including the standard *xrtpipeline* and the *Xspec* analysis tools. A logparabolic spectral model was systematically preferred for all observations. The MAXI data were taken from the public webpage and averaged over 1-day time bins.

The UVOT dataset comprised 59 exposures from MJD 55234 to 55247. Source counts were extracted from a 4.5° region around Mrk 421 and background counts from four same-sized neighbouring regions. Fluxes were computed using *uvotsource* with calibration, extinction and E(B-V) values from [2,3,4] respectively.

2. Correlated X-ray and GeV variability:

Figure 1 shows the *Fermi*-LAT lightcurve for a 24-day period surrounding the X-ray flare, with 1-day binning. There is a clear enhancement of the GeV flux, reaching a peak between MJD 55243 and 55245. Due to the poor statistics we were unable to test for variability in the spectral index on 1-day timescales. Instead, we identify three epochs based on the gamma-ray flux, as shown in Table 1, which we label *pre-flare*, *flare* and *post-flare* and calculate the spectrum for each. These spectra are presented in the next section and discussed in the context of the multi-wavelength observations.

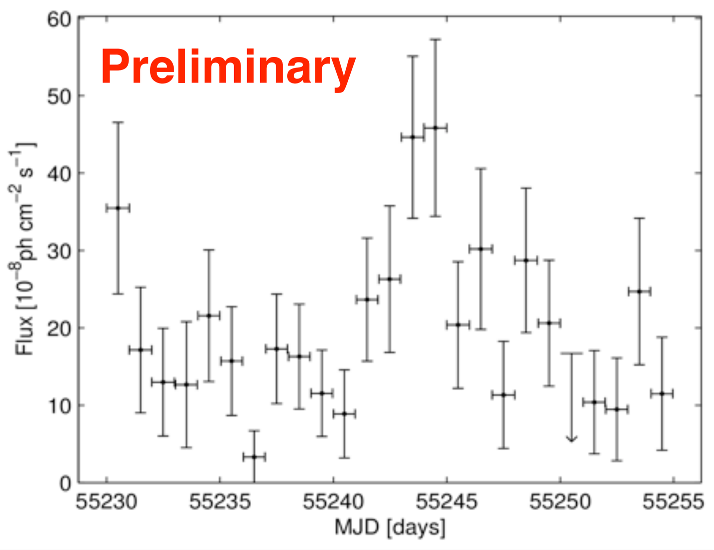

Fig. 1: Fermi-LAT gamma-ray lightcurve with 1-day binning.

Figure 2 shows the X-ray lightcurve from MAXI, with the same binning as in Figure 1. The X-ray flare is clearly visible, reaching a peak during MJD 55243, when the GeV flare was also at its highest.

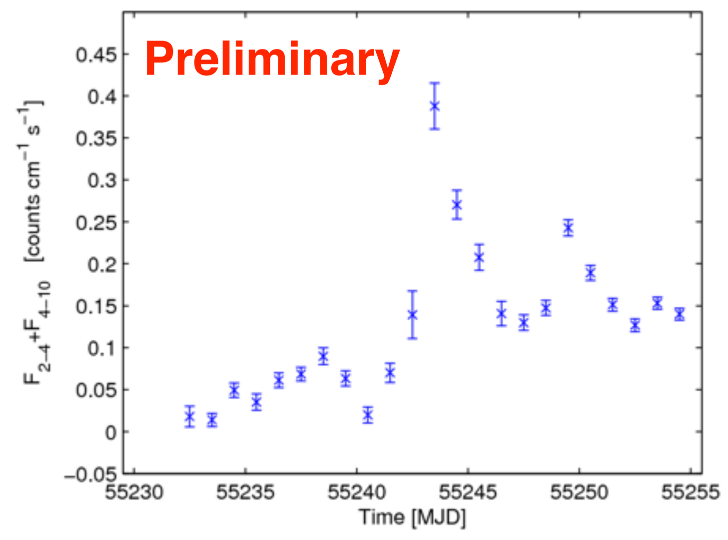

Fig. 2: MAXI X-ray lightcurve with 1-day binning.

The Pearson correlation coefficient between the two datasets is ρ=0.57, corresponding to an approximately 3σ detection of correlation between the GeV and X-ray fluxes, neglecting statistical errors (the p-value is 0.0041).

Table 1: Temporal periods defined by the GeV flux state around the flare.

Epoch	Start MJD	End MJD
Pre-flare	55238	55242
Flare	55242	55246
Post-flare	55246	55250

3. Spectral energy distributions:

The multiwavelength data were fit using the single-zone SSC model of [5]. For all three epochs, we assume a magnetic field B=0.01G and a Doppler factor δ=24 (see e.g. [6]). We model the electron distribution as a broken power law and we include an optical-UV contribution from the host galaxy using the model of [7].

For each of the *pre-flare* and *post-flare* epochs, two SEDs are derived. The solid curves were fit to the shape of the peak of the synchrotron emission in the X-rays (with the UVOT data providing an upper limit constraint) while matching the mid-point of the flux in the LAT band; the dotted curves were fit to the slope and flux in the LAT band, and the synchrotron peak was adjusted to match the peak of the X-ray data, without regard to the lower energy tail of the X-ray spectrum. For the *flaring* epoch (red curve), a single set of parameters was sufficient to fit the X-ray/GeV data.

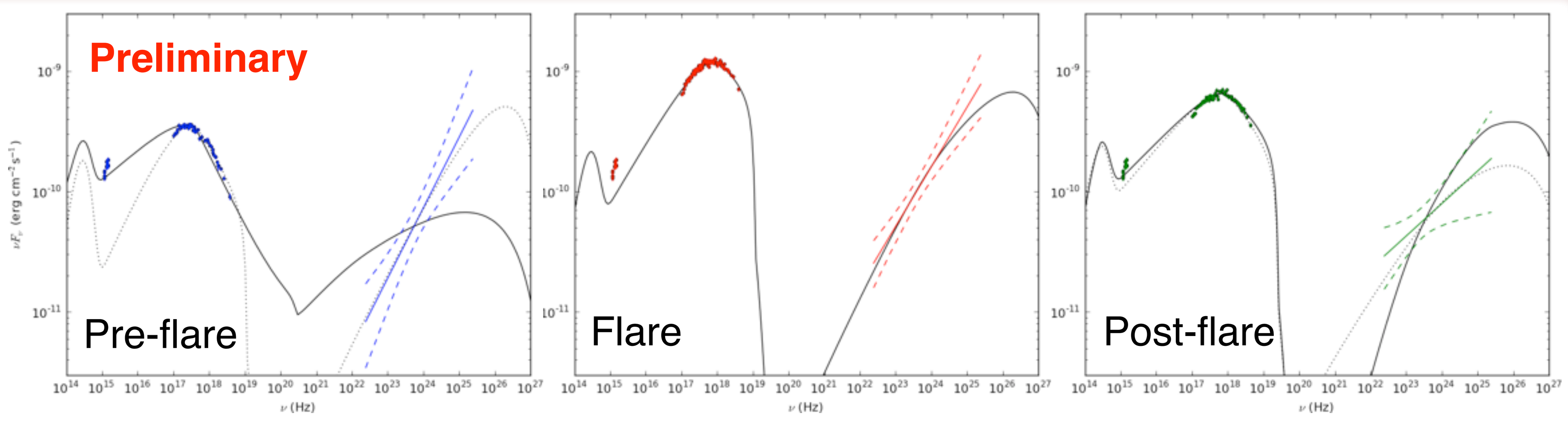

Fig. 3: Spectral energy distributions and one-zone SSC model predictions for the three epochs from simultaneous UVOT, XRT and *Fermi*-LAT observations.

Table 2: Parameters of SSC models shown in Figure 3. **Preliminary**

Epoch (curve)	γ_{break} (10^5)	p_1	p_2	n_e (cm^{-3})	R_b (10^{16} cm)	$R_b/c\delta$ (days)	u_B/u_E (10^{-3})
Pre-flare (solid)	4.0	2.5	4.2	0.34	4.62	0.76	5.0
Pre-flare (dots)	3.7	1.7	3.9	3.39	0.59	0.1	0.13
Flare	6.0	2.0	3.4	0.13	1.61	0.26	0.90
Post-flare (solid)	6.0	2.4	3.5	4.8E-03	2.03	0.33	5.2
Post-flare (dots)	6.0	2.3	3.7	2.8E-02	3.06	0.5	5.7

In the *pre-flare* epoch, the fit parameters for the X-ray-constrained (solid, left panel) and GeV-constrained (dotted, right panel) cases are sufficiently different that the overall SED cannot be described by a single zone model. The same is probably true for the *post-flare* epoch, though the differences in the physical parameters are less pronounced. The parameters of the SSC models for all epochs are given in Table 2.

4. Conclusions:

We have presented evidence for correlated variability of the GeV and X-ray emission on day-long timescales from the HBL Mrk 421 during an intense flare. Correlations between the X-ray and the Comptonized emission on such short timescales has previously only been detected in the TeV regime. Assuming a standard one-zone SSC paradigm, our observations establish a link between the low-energy electrons responsible for the GeV emission through the inverse-Compton process and the high-energy electrons radiating X-rays through the synchrotron process. When a one-zone SSC model is applied to the broad-band spectra for different flux states, only the period of the *flare* can be adequately modeled. One way that the discrepancy in the *pre-flare* and *post-flare* states might be resolved is to assume that multiple emission zones contribute to the flux during these epochs, whereas the *flaring* period is dominated simply by emission from a single zone. We conclude by noting the importance of all-sky X-ray and gamma-ray instruments, such as MAXI and the *Fermi*-LAT, without which short-timescale events such as this would likely go unnoticed.

References: [1] Abdo, A.A. et. al, 2011, arXiv:1108.1435, [2] Breeveld, A.A. et al., 2011, AIPC, 1358, 373, [3] Roming, P.W.A. et al., 2009, ApJ, 690, 163, [4] Schlegel, D.J. et al., 1998, ApJ, 500, 525, [5] Böttcher, M., & Chiang, J., 2002, ApJ, 581, 127, [6] Tramcere, A., et al., 2009, A&A, 501, 879, [7] Katarzyński, K., Sol, H., Kus, A., 2003, A&A, 410, 101